Harnessing Excess Photon Energy in Photoinduced Surface Electron Transfer between Salicylate and Illuminated Titanium Dioxide Nanoparticles

María A. Grela, Marta A. Brusa, and Agustín J. Colussi*

National Research Council of Argentina, P.O. Box 422, 7600 Mar del Plata, Argentina

Received: July 3, 1997; In Final Form: November 3, 1997[⊗]

Photons absorbed by nanocrystalline TiO_2 particles at 254 nm are found to be 7.7 times more efficient than those at 366 nm for driving the photocatalytic oxidation of salicylate S in aerated aqueous sols. The occurrence of this phenomenon is ascribed to the conjunction of (1) short diffusion times of photogenerated carriers to the surface of nanoparticles, a fact that allows chemical reaction to compete with energy relaxation, and (2) favorable donor $E_o(S^-/S^\bullet)$ redox potential and interfacial reorganization energy λ_R values, which make electron-transfer rates peak at energies inside the valence band of TiO_2. Master equation kinetic modeling shows that electron transfer from S into hyperthermal valence band holes takes place at rates consistent with $k_{sc} \sim 10^4$ cm s^{-1} at optimal exoergicity, if the excess energy is dissipated into the crystal lattice within a few picoseconds. Hydroxyl ions as donors would require much slower thermalization rates.

Introduction

Natural or artificial photosynthetic and photocatalytic systems that undergo sufficiently rapid charge separation may produce excited ion-radical intermediates upon broadband solar illumination.[1−4] The fundamental issue of whether the excess energy can be converted into chemical potential rather than being dissipated as heat—and therefore enhance the efficiency of such devices—remains, however, an open question and challenge.[1,5,6] Current understanding of the factors controlling interfacial electron transfer and carrier thermalization processes is insufficient to provide much guidance on how to achieve such goal. Since even formally endoergic charge transfers may occur at nonvanishing rates in a thermal bath,[7a,b] exploring the title issue necessarily involves accurate quantum yield measurements as function of irradiation wavelength, rather than searching for the onset of supraband-edge redox reactions.[8] The photocatalytic oxidation of salicylate S in clear TiO_2 sols seems appropriate as a case study because (1) the short diffusion times of photogenerated carriers to the surface of nanoparticles may undercut their equilibration with the environment[9] and (2) S can tightly bind to TiO_2 surfaces[10]—the semiconductor of choice in many practical applications—a condition expected to maximize interfacial electronic coupling and transfer rates. We found that quantum yields actually increase significantly with excess photon energy over the bandgap, $E^* = E_\lambda - E_{bg}$, and reach a plateau at ca. $E^* \sim 0.9$ eV. We show that this is evidence of a redox reaction that undergoes its transition from the normal to the inverted Marcus region while competing with excited hole relaxation within the valence band of TiO_2. A master equation kinetic analysis of experimental results reveals that hot carrier thermalization in the picosecond time range implies that interfacial electron transfer between salicylate and polycrystalline TiO_2 nanoparticles takes place with rate constants approaching $k_{et} = 2 \times 10^{-15}$ cm^4 s^{-1} at optimal exoergicity.

Experimental Section

Scattered radiation losses—a pervasive complication in quantitative photochemistry of colloidal systems—were minimized in visually clear sols prepared by exhaustive ultracentrifugation (20 min at 9770 *g*) of previously sonicated (15 min at 35 kHz, 100 W) 2 g/L TiO_2 (Ecolinc, 76% anatase−24% rutile) slurries in 1 mM PO_4H_2Na.[11] The UV absorption spectra of the stable sols thus obtained, recorded with an integrating sphere accessory (Hitachi U-3210 model, 60 mm sphere diameter, opening ratio: 7.8%), are shown in Figure 1. They confirm that quadratic extrapolation of the baseline below 380 nm provides a correct appraisal of scattered radiation in standard absorption spectra of these colloids, as previously suggested.[11] The onset of absorption at 380 nm rules out quantum size effects.[12] Atomic force microscopy (PSI) of sol samples dried on mica holders reveals the presence of fine particles (diameter ≤ 5 nm), interspersed with a few larger (∼15 nm) aggregates. Air-saturated sols (3 cm^3, $[TiO_2] \sim 1-3$ mM, absorbance ≤ 0.3 cm^{-1}, $[O_2] = 0.3$ mM, pH ∼ 4.5) contained in square prismatic cells were fully illuminated with monochromatic radiation (from

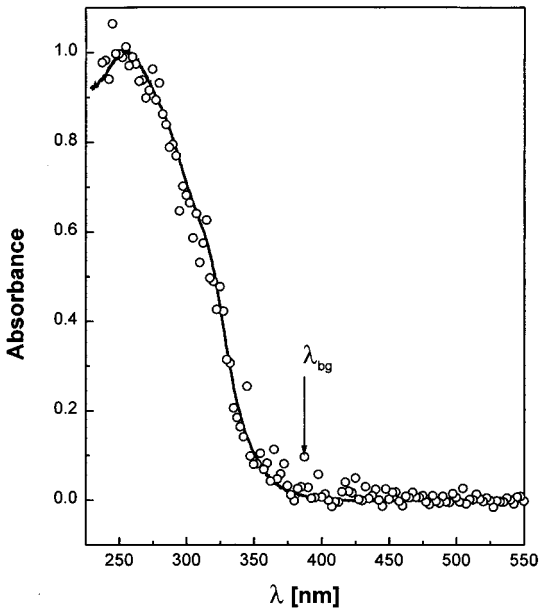

Figure 1. Normalized absorption spectrum of TiO_2 sols. Circles: obtained with an integrating sphere accessory. Solid curve: standard transmission spectrum corrected for scattering by quadratic extrapolation of the baseline below 400 nm.[11] The onset of absorption at $\lambda_{bg} \sim 380$ nm—close to literature values for the bandgap energy in bulk TiO_2—rules out quantum size effects.[12]

* Corresponding author. E-mail: ajcoluss@cco.caltech.edu.

[⊗] Abstract published in *Advance ACS Abstracts,* December 1, 1997.

S1089-5647(97)02172-X CCC: $14.00

a Kratos-Schoeffel monochromator, ±5 nm bandwidth)[11] at several wavelengths in the presence of variable [S]'s (pK_{SH} = 2.9). The spectra of these colloidal suspensions proved to be linear superpositions (within 2%) of separate TiO_2 and S spectra, i.e., we found no evidence of the formation of red-shifted charge-transfer complexes between S and nanocrystalline TiO_2 particles suspended in 1 mM phosphate buffers below [S] ~ 70 μM.[13] Constant (up to 50% conversion) salicylate decay rates R_{-S} were determined by HPLC [Spherisorb (Sigma) ODS-2 5 μm, methanol:water 1:20]. The combined yields of 2,3- and 2,5-dihydroxybenzoic acid DHB, the identifiable reaction products, amount to (49 ± 4)%. The remainder of S losses is ascribed to the formation of (CO_2 + H_2O), concurring with previous reports.[14] We verified that this stoichiometry is independent of λ or [S], and that the extent of S photodecomposition in TiO_2-free solutions is negligible. Absorbed photon fluxes I_a at each wavelength were calculated from incident photon fluxes I_o (typically within the $10^{14}-10^{15}$ photons cm^{-2} s^{-1} range, as determined in situ using the phenylglyoxylic acid actinometer)[11] and experimentally determined TiO_2 absorbances. They were varied 20-fold at each wavelength by attenuating the beam and by diluting the TiO_2 sols.

Results and Discussion

Reproducible quantum yields for S decomposition, calculated as $\phi_{-S} = R_{-S}/I_a$, are shown in Figure 2. It is apparent that ϕ_{-S} increases between 3.8 and 6.4 times from 366 to 254 nm, depending on [S]. Figure 3 registers linear ϕ_{-S}^{-1} vs $[S]^{-1}$ dependences, typical of saturation kinetics. In accord with previous results and considerations, R_{-S} was found to be linearly dependent on I_a (Figure 4), confirming first-order carrier losses in the ranges investigated.[11,15] The above results respond to the following scheme:

$$h\nu \rightarrow e_{cb} + h_{vb}^* \quad (1)$$

$$h_{vb}^* + S \rightarrow X \quad (2)$$

$$\beta h_{vb}^* + X \rightarrow (DHB + CO_2 + H_2O, \text{etc}) \quad (3)$$

$$h_{vb}^* \rightarrow \text{loss} \quad (4)$$

$$(e_{cb} + O_2 \rightarrow O_2^{\bullet -}) \quad (5)$$

where h_{vb}* stands for hot valence holes (see below) and X for reactive surface intermediates; β is the average number of holes consumed in the oxidation of the latter. Thermalized electrons e_{cb} are assumed to be slowly scavenged by O_2.[11,15] This mechanism leads to

$$\phi_{-S}^{-1} = (1 + \beta) + (k_4/k_2)\,[S]^{-1} \quad (6)$$

with $(1 + \beta) \leq 15.3$. The latter condition follows from the fact that formation of DHB in step 3 requires a one-electron oxidation, while (CO_2 + $3H_2O$) are in principle the end products of a 27-electron oxidative sequence, i.e.: $\beta \leq 0.49 + 27(1 - 0.49) = 14.3$. Figure 3 confirms that (1) slopes—i.e.; $\langle k_2/k_4 \rangle$, the average ratios of charge transfer to terminating pathways for h_{vb}*—are increasing functions of $E_\lambda = hc/\lambda$ and that (2) $(1 + \beta) = 13.8 \pm 2.0$ is independent of λ and close to the expected value. In other words, the full oxidation of S into (CO_2 + H_2O) is photochemically driven with, perhaps, a marginal participation of dark reactions involving O_2 or the products of its partial reduction. Therefore, the limiting yields $\phi_{-S}([S] \rightarrow \infty) = (1 + \beta)^{-1} = 0.068$ are not really imposed by reactive carrier losses but by the reaction stoichiometry because the X-intermediates consume carriers otherwise available for S oxidation. For example, although $\phi_{-S} = (4.5 \pm 0.3)\%$ at [S] = 67 μM, 254 nm, we estimate that 63% of the photons absorbed by TiO_2 nanoparticles are actually utilized to drive degradative reactions 2 and 3 in this system. The ensuing analysis focuses on the wavelength dependence of ϕ_2, the specific quantum yield of S oxidation: $\phi_2^{-1} = 1 + (k_4/k_2)\,[S]^{-1} = \phi_{-S}^{-1} - \beta$, which increases almost 8-fold between 366 and 254 nm.

Conservation of linear momentum dictates that the excess kinetic energy is partitioned among carriers depending on their relative masses, i.e., $E_h^* = E^*\,[1 - m_{h(ole)}/m_{e(lectron)}]$. Since $m_h/m_e \leq 0.08$ for TiO_2,[9] any excess energy is fully channeled

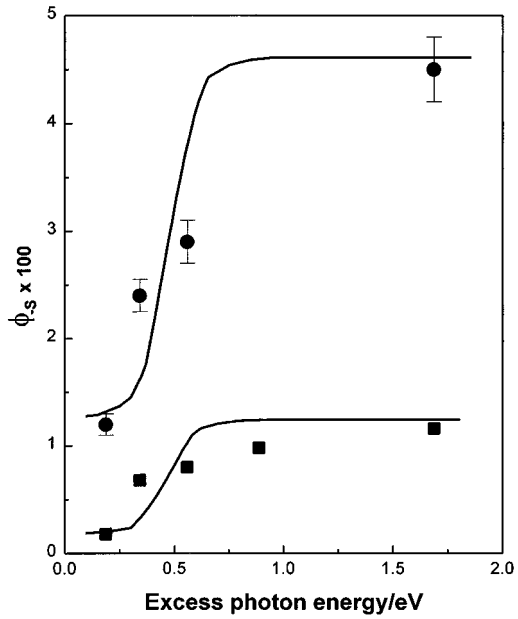

Figure 2. Quantum yields of the photocatalyzed oxidation of salicylate ϕ_{-S} vs excess photon energy. Excess photon energy calculated as $E^* = hc(\lambda^{-1} - \lambda_{bg}^{-1})$. Circles: [S] = 66.7 μM. Squares: [S] = 8.32 μM. Solid lines calculated by integration of a 32-level master equation model based on Scheme 1 (see text).

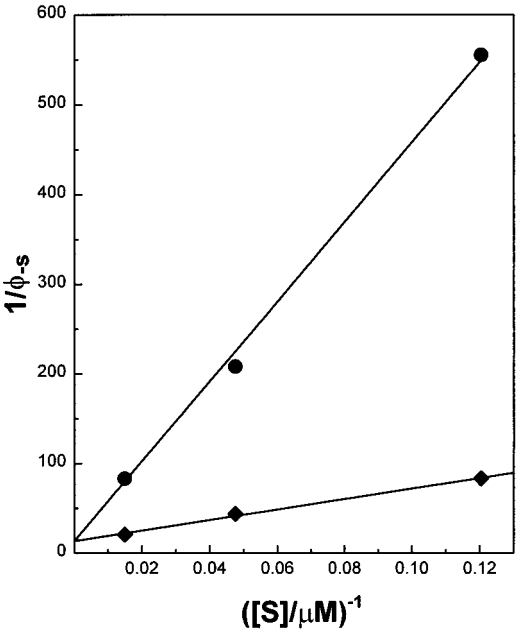

Figure 3. Stern−Volmer plots of ϕ_{-S}^{-1} vs $[S]^{-1}$. Circles: λ = 366 nm. Diamonds: 254 nm. A common intercept at 13.5 ± 2.0 implies a λ-independent stoichiometry and the competition of salicylate with more reactive intermediates for excited holes on the surface of TiO_2 nanoparticles. Slopes represent the average ratio of termination to charge-transfer rate constants $\langle k_4/k_2 \rangle$.

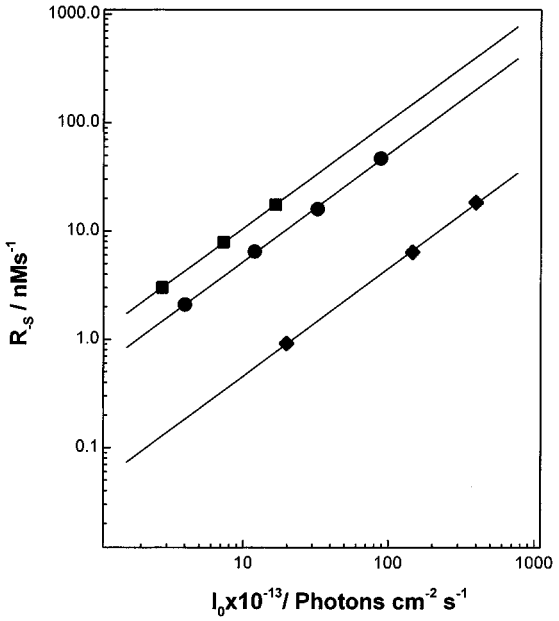

Figure 4. Salicylate decay rates R_{-S} vs incident photon fluxes I_0 in TiO_2 sols, $[S]_0 = 66.7$ μM. Squares: $\lambda = 254$ nm. Circles: 330 nm. Diamonds: 366 nm. Slopes, $n = \log R_{-S}/\log I_0$, are unitary within experimental error.

into the valence band hole. The first relaxation phase for photoexcited carriers involves thermal equilibration of the initially generated carrier with its background congeners. This redistribution of excess energy takes place within 10−100 fs, a process that can be hardly intercepted by interfacial charge transfers.[1,6] Therefore, the hot carriers implicated in steps 2 and 3 are assumed to be excited holes h_{vb}* that react while cooling to room temperature by interaction with the crystal lattice.[16] In accord with this view, the action spectrum of Figure 2 can be quantitatively accounted for by a master equation approach over a discrete manifold (cf. Scheme 1)

$$dn_{max}/dt = I_{a,max} - (k_{2,max}[S] + k_{max\rightarrow max-1})n_{max} \quad (7)$$

$$dn_i/dt = I_{a,i} - (k_{2,i}[S] + k_{i\rightarrow i-1})n_i + k_{i+1\rightarrow i}\, n_{i+1} \quad (0 < i < n_{max}) \quad (8)$$

$$dn_0/dt = I_{a,0} - (k_{2,0}[S] + k_t)n_0 + k_{1\rightarrow 0}n_1 \quad (9)$$

where n_i is the hole population of level i and n_{max} the level reached by 254 nm photons. Notice that (1) the first term of the right-hand side of eqs 7−9 vanishes unless monochromatic radiation of matching energy directly populates level i, and (2) it is reasonable to omit endothermic ($i \rightarrow i + 1$) transitions because the temperature of the hot carriers is much larger than that of lattice. Excited holes, $h_{vb}* = h_{vb}(E_j*)$, accept electrons from salicylate S with rate constants $k_{2,j}$ given by[7a,b]

$$k_{2,j}(E^*) = A_2 \exp\{-(E_j^* + E_{vb} - E_0 - \lambda_R)^2/4\lambda_R k_B T\} \quad (10)$$

or cascade down with energy-dependent deactivation rate constants, $k_{j\rightarrow i} = k_{1\rightarrow 0}E^*_j$,[6,8b] prior to termination from the ground level with k_t. E_0 is the standard oxidation potential of the $S^-/S^\bullet$ couple on the TiO_2 surface, and λ_R is the reorganization energy.[7a,b] The best fit is obtained with $E_0(S^-/S^\bullet)_{surface} = 3.14$ V (vs NHE), $A_2 = 1.5 \times 10^{13}$ M^{-1} s^{-1}, $k_{1\rightarrow 0} = 2 \times 10^{11}$ s^{-1}, $k_t = 1.9 \times 10^7$ s^{-1},[11,15] and $\lambda_R = 0.575$ eV, i.e., about half of normal values for homogeneous electron-transfer reorganization energies.[7c,17] As expected, the critical parameters are E_0 and λ_R. The actual value of $k_{1\rightarrow 0}$ is obviously tied up to the assumption that deactivation rate constants increase linearly with E* in nanocrystalline TiO_2.[6] We adopted $E_{vb} = 3.03$ V, considering that at low photon fluxes sol particles remain neutral at their flatband potentials.[20] $E_0(S^-/S^\bullet)_{surface} = 3.14$ V is very close to the value for the related (SH/SH^+) couple derived from Eberson's relationship, $E_0(SH/SH^+) = 0.78 \times IP(SH) - 4.26 = 2.96 \pm 0.2$ V (vs NHE),[18,19] with IP(SH) = 9.26 eV.[20] From this perspective, the fact that the inverted region—which is certainly reached because $E^*(\lambda = 254\ nm) = 1.7\ eV \gg \lambda_R \sim 0.58$ eV—is not reflected in decreasing ϕ_{-S} values at sufficiently short wavelengths is due to efficient deactivation of highly excited carriers to the energy range that sustains the fastest electron-transfer rates, i.e., those at the top of the Marcus parabola. If deactivation were slow enough, quantum yields would decline above a certain excess energy. If hot carriers take much longer to reach the interface, as it will occur within macroscopic phases, competition is defeated. A similar analysis reveals that although OH^- oxidation yields—with $E_0(H_2O/OH^\bullet) = +2.53$ V at pH = 4.5,[22] $\lambda_R > 1.0$ eV—also increase with E* and display an inflection point at $E^* \sim 0.5$ eV (cf. Figure 2), the expected enhancement only amounts to ∼20% between 366 and 254 nm, unless thermalization rates were about 10 times smaller. On this basis, our data seem to rule out a major contribution of H_2O oxidation to salicylate decay, particularly at the shortest wavelengths. Further studies on this issue are underway. For particles of 2.5 nm average radius, surface area $A_p = 7.8 \times 10^{-13}$ cm^2, we calculate $k_{sc} = A_2/A_p = (1.5 \times 10^{13}/7.8 \times 10^{-13}/\ 6 \times 10^{20}) = 3.2 \times 10^4$ cm s^{-1}, in good accord with semiclassical estimates of the upper limit to the rate constant for electron transfer at semiconductor−liquid interfaces.[23,24] From $n_p = 1$ hole (particle)$^{-1} = 1.5 \times 10^{19}$ cm^{-3}, we formally obtain $k_{et} = k_{sc}/n_p = 2 \times 10^{-15}$ cm^4 s^{-1}.[24] The relevant dynamic implication is that *electron-transfer processes can effectively compete with hot carrier thermalization in the picosecond time scale on nanoclusters*[16] *and that such events can be modeled using realistic parameters and assumptions*.

SCHEME 1:

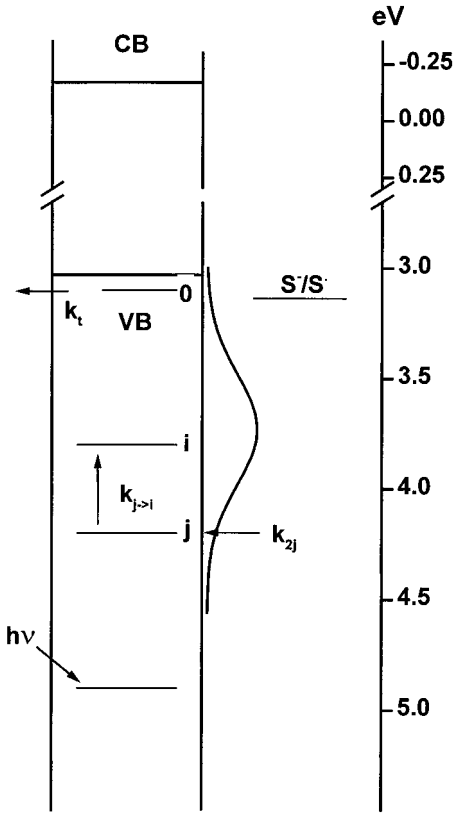

Our calculations predict that although shorter wavelength photons are slightly more efficient on an absolute basis, 300 nm photons are the most economical—i.e., lead to the largest (moles of salicylate decomposed/unit energy) ratio—for accomplishing the photocatalytic oxidation of dilute S solutions, a useful consideration in water decontamination technology.[21] It is apparent that (1) irradiation wavelength is a critical parameter in photochemical studies on colloids, and (2) it is unwarranted to assume thermal photochemistry in heterogeneous microenvironments.[2b]

Present results contrast with transient grating studies on single-crystal *n*-TiO_2 (001)/H_2O interfaces by Kasinski et al., in which electrons were largely transferred from OH^-_s into cold carriers.[25] As pointed out above, the larger surface-to-volume ratio in nanoparticles, the matching E_0, λ_R, and E_{bg} values for S and TiO_2, respectively, and the fact that S is a bidentate ligand that can interact covalently to TiO_2 may underlie the dissimilar responses.[26] Ross and Nozik have shown that solar energy could be converted into chemical potential with 66% efficiency by single-threshold semiconductor devices[5]—i.e., twice the maximum efficiency of an ideal thermal conversion device—if excited carriers would react with interfacial species prior to equilibrating with the environment. Our results provide the first direct experimental evidence, based on wavelength-dependent quantum yields, that the latter condition can be approached in appropriately designed systems.[27]

Acknowledgment. This project was financially supported by the National Research Council of Argentina (CONICET) under Grant PID1131/91.

References and Notes

(1) (a) Miller, D. J. R.; McLendon, G. L.; Nozik, A. J.; Schmickler, W.; Willig, F. *Surface Electron Transfer Processes*; VCH Publishers: New York, 1995; Chapter 4. (b) Meisel, D. In *Semiconductor Nanoclusters*; Kamat, P. V., Meisel, D., Eds.; Surface Science and Catalysis 103; 1996; pp 79−97.

(2) (a) Wiederrecht, G. P.; Niemczyk, M. P.; Svec, W. A.; Wasielewski, M. R. *J. Am. Chem. Soc.* **1996**, *118*, 8. (b) Kirmaier, C.; Laporte, L.; Schenck, C. C.; Holten, D. *J. Phys. Chem.* **1995**, *99*, 8910.

(3) (a) Wang, Y. *Adv. Photochem.* **1995**, *19*, 179. (b) Weller, H.; Eychmüller, A. *Adv. Photochem.* **1995**, *20*, 165. (c) Anderson, C.; Bard, A. J. *J. Phys. Chem.* **1997**, *101*, 2611. (d) Hagfelt, A.; Grätzel, M. *Chem. Rev.* **1995**, *95*, 49.

(4) Nozik, A. J.; Memming, R., *J. Phys. Chem.* **1996**, *100*, 1306 and references therein.

(5) Ross, R. T.; Nozik, A. J. *J. Appl. Phys.* **1982**, *53*, 3813.

(6) Nozik, A. J.; Turner, J. A.; Peterson, M. W. *J. Phys. Chem.* **1988**, *92*, 2493.

(7) (a) Marcus, R. A. *Angew. Chem., Int. Ed. Engl.* **1993**, *32*, 1111. (b) Marcus, R. A. *J. Chem. Phys.* **1965**, *43*, 679. (c) Bahnemann, D. W.; Hilgendorff, M.; Memming, R. *J. Phys. Chem.* **1997**, *101*, 4265.

(8) (a) Rosenwaks, Y.; Hanna, M. C.; Levi, D. H.; Szmyd, D. M.; Ahrenkiel, R. K.; Nozik, A. J. *Phys. Rev. B*, **1993**, *48*, 14675. (b) Cooper, G.; Turner, J. A.; Parkinson, B. A.; Nozik, A. J. *J. Appl. Phys.* **1983**, *54*, 6463.

(9) Enright, B.; Fitzmaurice, D. *J. Phys. Chem.* **1996**, *100*, 1027.

(10) Tunesi, S.; Anderson, M. *J. Phys. Chem.* **1991**, *95*, 3399.

(11) Grela, M. A.; Coronel, M. E. J.; Colussi, A. J. *J. Phys. Chem.* **1996**, *100*, 16940.

(12) Nozik, A. J. *Photocatalytic Purification and Treatment of Water and Air*; Ollis, D. F., Al-Ekabi, H., Eds.; Elsevier Science Publishers: Amsterdam, 1993; p 39.

(13) Moser, J.; Punchihewa, S.; Infelta, P. P.; Grätzel, M. *Langmuir* **1991**, *7*, 3012. Salicylate markedly red-shifts the absorption spectra of hydrolytic TiO_2 colloids *in the absence of competing ligands*.

(14) (a) Mills, A.; Holland, C. E.; Davies, R. H.; Worsley, D. *J. Photochem. Photobiol. A* **1994**, *83*, 257. (b) Mathews, R. W.; McEvoy, S. R., *J. Photochem. Photobiol. A* **1992**, *66*, 355.

(15) (a) Grela, M. A.; Colussi, A. J. *J. Phys. Chem.* **1996**, *100*, 18214 and references therein. (b) Schwarz, P. F.; Turro, N. J.; Bossmann, S. H.; Braun, A. M.; Wahab, A. A.; Dürr, H. *J. Phys. Chem. B* **1997**, *101*, 7127.

(16) Shank, C. V.; Fork, R. L.; Laheny, R. F.; Shah, J., *Phys. Rev. Lett.* **1979**, *42*, 112.

(17) Grätzel, M. *Heterogeneous Photochemical Electron Transfer*; CRC Press: Boca Raton, FL, 1988.

(18) (a) Eberson, L. *Adv. Phys. Org. Chem.* **1982**, *18*, 79. (b) Eberson, L. *Electron Transfer Reactions in Organic Chemistry*; Springer-Verlag: New York, 1987. An earlier, less positive value, $E_0(S^-/S^\bullet) = +1.24$ V,[19] obtained by polarography fails to qualify as the thermodynamically reversible redox potential required in eq 10, as discussed at length by Eberson.

(19) Suatoni, J. C.; Snyder, R. E.; Clark, R. O. *Anal. Chem.* **1961**, *33*, 1895.

(20) NIST Standard Reference Database 25, version 2.02; National Bureau of Standards and Technology: Gaithersburg, MD, 1994.

(21) Bahnemann, D.; Cunningham, J.; Fox, M. A.; Pelizzetti, E.; Pichat, P.; Serpone, N. In *Aquatic and Surface Photochemistry*; Helz, G. R., Zepp, R. G., Crosby, D. G., Eds.; Lewis Publishers: Boca Raton, FL, 1994; Chapter 21 and references therein.

(22) Latimer, W. M. *Oxidation Potentials*, 2nd ed.; Prentice-Hall: Englewood Cliffs, NJ, 1952; p 48.

(23) Smith, B. B.; Halley, J. W.; Nozik, A. J. *Chem. Phys.* **1996**, *205*, 245.

(24) Lewis, N. S. *Annu. Rev. Phys. Chem.* **1991**, *42*, 543.

(25) Kasinski, J. J.; Gomez-Jahn, L. A.; Faran, K. F.; Gracewski, S. M.; Miller, R. J. D. *J. Chem. Phys.* **1989**, *90*, 1253.

(26) Rehm, J. M.; McLendon, G. L.; Nagasawa, Y.; Yoshihara, K.; Moser, J.; Grätzel, M. *J. Phys. Chem.* **1996**, *100*, 9577.

(27) Koval, C. A.; Torres, R. *J. Am. Chem. Soc.* **1993**, *115*, 8368.